Power Unavailability Reduction in Distribution Grid Fault Management with Entropy Minimization

Michele Garau
Department of Energy Systems
SINTEF Energy Research
Trondheim, Norway
michele.garau@sintef.no

Bjarne E. Helvik
Dept. of Information Security and Communication Technology - NTNU
Trondheim, Norway
bjarne@ntnu.no

***Abstract*—Smart automation is acquiring a high importance in current distribution systems. The high number of buses, the radial topology, the small number of sensors and automated devices, require new approaches in managing fault conditions. These approaches must be able to deal with a high level of uncertainty of the state of the system and the measurement data. In this paper a novel method for fault location and isolation is proposed, which is based on the principle of entropy minimization. The algorithm builds a switch operation strategy which is able to locate the fault in a minimum number of manoeuvres, and therefore to reduce the impact of blackouts in terms of power unavailability. The application of the method on different distribution network topologies, with different levels of automation in terms of fault indicators and remotely controlled switches, demonstrates the potential of the method for distribution system analysis and supporting system automation planning.**

***Index Terms*—Power grid availability, Smart Grid, Distribution System Protection, Reliability Modelling**

I. Introduction

Nowadays, distribution systems are acquiring a high attention in current power systems. The spread of low size generation power plants among domestic appliances, the increasing interest towards electricity as energy vector for different usages (buildings heating and cooling with heat pumps, electric vehicles transportation, etc.), the trend towards an horizontal participation to the energy market, increase the necessity of new solutions that enhance the quality of service of the power system at the distribution level.

In this scenario, the reliability of distribution networks assumes a paramount importance. To minimize the impact of outages among distribution network customers, it becomes fundamental to introduce smart automation that allows a fast detection, location and isolation of network faults, and to elaborate strategies for a quick restoration of the network. In fact, currently in Europe about 80% of the blackouts are due to faults that occur on the distribution grid, and the yearly average blackout duration ranges from 15 to 400 minutes per customer, mostly due to the weak automation of distribution systems which makes fault location mostly a process based on grouping of customer outage calls and experience-based power lines patrolling. [1]. In this context, this paper proposes a novel, efficient method to locate and isolate faulted line segments in distribution networks, and minimize the unavailability of the power supply to the unaffected part of the network, i.e., restoring it in a minimum time. Both these two objective formulations will be used synonymously in the paper.

Traditionally, fault location methods are developed for processing the raw *data* generated from specific measurement devices and returning possible fault locations, with a specific level of uncertainty. Essentially, these methods are meant to provide a useful *information* to Distribution System Operators (DSOs) that, upon this information, will build a plan for inspecting the network and reduce the overall sectioning and repairing time, isolating the fault and restoring the power supply on the healthy portion of the network. Fault isolation and service restoration can be considered as processes that lay on top of the *data-information* stack, which elaborate a strategy for network inspection in failure conditions; this stage of fault management typically relies on a solid empirical knowledge of the power system. The automation of this process allows to extend the *knowledge* of the system, by elaborating an optimal isolation and restoration strategy that takes into account different factors, e.g. the accuracy of measurement data and the consequent uncertainty in the information elaborated by the fault location algorithms, and provides a fundamental support to DSOs in decision making during fault conditions (Fig. 1).

In transmission systems different techniques have been developed and successfully applied for allowing an efficient and fast location of faults along the network. However, these techniques may not directly be applied in distribution systems. The high number of buses, often weakly monitored and automated, and the high number of lateral branches, make the application of transmission system fault location techniques to distribution networks unsuited. Achieving in distribution systems a level of monitoring comparable with transmission systems would require a massive investment. For this reason, in the last decades a large number of works have focused on formulating new methodologies for fault location that are specific for distribution networks [2], [3]. Despite being purposely designed for distribution systems, these methods

This paper has been funded by CINELDI - Centre for intelligent electricity distribution, an 8 year Research Centre under the Research Council of Norway's FME-scheme (Centre for Environment-friendly Energy Research, 257626/E20). The authors gratefully acknowledge the financial support from the Research Council of Norway and the CINELDI partners.

This is the accepted version of an article published at 2021 5th International Conference on System Reliability and Safety (ICSRS)
http://dx.doi.org/10.1109/ICSRS53853.2021.9660625

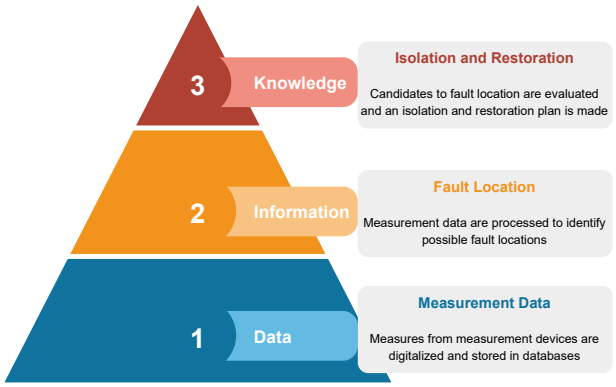

Fig. 1. Data processing levels in Fault Location, Isolation and Service Restoration process

still heavily rely on a high volume of measurement data from the distribution network. Moreover, these methods provide little support to DSOs in managing the fault condition. These methods in fact basically aim at processing the raw *data* to elaborate accurate *information* regarding a possible fault location (see Fig. 1). In this context, the strategy for optimally isolate the faulted network section and restore the power supply to the healthy part of the network is left upon the knowledge and experience of distribution network operators.

Few works have proposed methods that take into account measurement data uncertainty in fault location and isolation processes in a integrated way, in order to support DSOs' *knowledge* in fault management interventions planning (Fig. 1). In [4], Hermansen et al. present a methodology that uses event tree analysis and simulates the switching sequence that minimizes the potential interruption costs for each fault location. The methodology is based on Bayes-updating of fault location probabilities during a disconnectors switching sequence, considering possible Fault Indicators inaccuracies. In [5] an integrated methodology for fault location and isolation is proposed, which is based on Markov Decision Process. It takes into account uncertainties of fault indicators and optimizes different interests, such as the minimization of interruption time, importance of the load and the number of switch manipulations. In both these works, scalability of the methods and computational efficiency are not yet investigated.

A. Contribution and organization of the paper

In this paper a novel method for fast fault location and isolation is proposed. The algorithm exploits the concept of entropy minimization to build a binary decision tree. This tree is meant to support the switches operation strategy and locate and isolate the fault in a minimum number of manoeuvres. Timing in operating disconnector switches and imperfect short circuit fault indicators are taken into account. The method is applied to a radial distribution network. Different network topologies will be studied and compared in terms of power unavailability, more specifically in terms of average fault location and isolation time and fault outage time, with varying automation configurations. The approach is aimed at being so computationally efficient that it allows to be exploited for iterative planning of switches and fault indicators placement.

The paper is organized as follows. In Section II the basics of entropy theory is presented. Section III introduces the fundamental assumptions, notation and metrics adopted. Section IV presents the entropy method for distribution network fault location. This is extended to the case where fault indicators are installed in Section V. The application of the method is exemplified in Section VI with a simple distribution network. In Section VII the method is used to study different reference distribution networks. Section VIII concludes the paper with final considerations, remarks and potential future works.

II. Basic principles of entropy theory

In thermodynamics, the entropy provides a quantitative measure of the disorder of a system in a specific state. In information theory, the entropy is a quantitative measure of information, having an analogous interpretation. The larger the uncertainty of the outcome of an information transfer, the larger is the information associated with it. If a specific outcome x with probability p_x is regarded, the associated information is defined as $-\log_2(p_x)$. A definite outcome, $p_x = 1$, provides no information, while the information goes toward infinity as $p_x \to 0$. The expected information of all outcomes are defined as the entropy. Formally, if the outcome is represented by a stochastic variable X, the entropy is:

$$\mathscr{E}(p_X) = -\sum_{x \in X} p_x \log_2(p_x) \tag{1}$$

A detailed definition of entropy and its properties can be found in [6]. One important property of the entropy from information theory states that the entropy of X represents the minimum average number of bits required to establish the outcome of X [7]. This property can be restated by asserting that the entropy represents the lower bound of the average number of inspections needed to identify a random variable of a set with probability of occurrences p_X [8]. If we assign the attributes $A_X = \{A_x\}_{x \in X}$ to the elements X in the inspection process, where $A_x \in \{0,1\}$, the optimal binary inspection at a given stage is the one that minimizes the entropy, i.e. that maximizes the information gain W:

$$\begin{aligned} W(X,A_X) = \mathscr{E}(p_X) - \mathscr{E}(p_{X|A_x=1}) \sum_{\forall x: A_x = 1} p_x \\ - \mathscr{E}(p_{X|A_x=0}) \sum_{\forall x: A_x = 0} p_x \end{aligned} \tag{2}$$

This method, called ID3 algorithm [9], is a greedy heuristic approach that supports the generation of binary decision trees that are globally near-optimal in a large number of settings with efficient computational cost [10].

III. Notation and basic relations

A. Assumptions

A radial power distribution network is regarded. Each link of the network connecting two buses consists of a disconnector switch (hereafter called *switch* for simplicity), which may

This is the accepted version of an article published at 2021 5th International Conference on System Reliability and Safety (ICSRS)
http://dx.doi.org/10.1109/ICSRS53853.2021.9660625

be followed by fault indicator, then followed by a power distribution line and/or a load. Fault indicators are considered as sensors able to provide a signal whenever a fault overcurrent (short circuit) is detected downstream of the fault indicator location. The following assumptions are considered:

1) The customers connected to the network are passive, i.e. the fault current is injected by a single source located at the distribution substation.
2) An arbitrary number of lines is equipped with fault indicators. The information gathered by fault indicators is characterized by a given uncertainty.
3) The network may be equipped with an arbitrary number of fault protection devices (breakers or fuses) with proper time-current selectivity. The remaining switchgears are switches. Each of these may either be manually controlled or remotely operated. Both protection devices, and manually and remotely operated switches, are considered as fault-free, i.e. the operation over the switch always returns into a physical disconnection or reconnection of the circuit.

B. Network topology

The structure of the network as well as the relation between switches, and the relation between distribution lines and loads, may be represented by a tree-shaped directed graph G, where the direction follows the power flow. The vertices represent what in the following are referred to as *elements*, i.e. network components (i.e. lines and loads) that may cause a network service disruption when they fail. The number of vertices is denoted m. Without loss of generality, the root vertex is indexed 1, the remaining $2,\dots,m$. In addition, a network branch may have a failure indicator placed with the switch, which indicates if a failure has occurred in the downstream network. This will be dealt with in section V.

Let $K_i, i = 1,\dots,m$ be a vector of length m where

$$K_{ij} = \begin{cases} 1 & \text{There is a path from } i \text{ to } j \text{ in } G \\ 0 & \text{Otherwise} \end{cases} \tag{3}$$

K_i represent the elements that receive the downstream power flow through i. $K = \{K_1,\dots,K_m\}^T$ is then a matrix representing the downstream power flow. If $\mathscr{A}_G$ is the adjacency matrix of the directed graph G, K is straightforwardly obtained as the vertices that may be reached in a number of steps equal to the length of the longest path in the tree, $\mathscr{D}_G$, plus itself. Hence,

$$K = \sum_{i=1}^{\mathscr{D}_G} \mathscr{A}_G^{\cdot i} + I_m \tag{4}$$

where $x^{\cdot i}$denotes the i fold matrix product and I_m is the identity matrix of size m. For notational convenience, we also define the elements that do not receive the downstream power flow through i as $\overline{K}_i = 1 - K_i$.

C. Failure and recovery characteristics

Switches are assumed to be fault free. For the reliability analysis, it is also assumed that elements fail and that at most one element is failed at a time. Each element i in the system has two parameters: λ_i, fault intensity and r_i, expected fault repair time. The vector representations of these are λ and r.

Fault localization time is calculated and associated with each element. The following times are regarded:

- Localization time l_i: the time to locate and isolate the fault when element i has failed.
- Outage time l_{ij}^*: the time from the instant when element i fails until element j may be put into unstable operation. By unstable operation it is meant that element j may be powered, but the fault location process is still ongoing, therefore further interruptions may occur.

How to obtain these will be discussed in Subsection IV-B. The corresponding vector and matrix are denoted l and L^*, respectively. From the definitions, it is seen that $l = L^* \cdot I_m$ and that $l_{ij}^* \leq l_i$.

D. Switch operation times

The switches $2,\dots,m$, may be remotely or manually operated. Remotely operated switches are characterized by a short operation time δ. The set of remotely operated switches is denoted ρ. For the manually operated switches, the operation time is given by the travelling time d_{ij} between switches i and j. It is assumed that $\delta \ll d$. Hence, remotely controlled switches are always operated before the manual operation starts. Accordingly, we build the following switch interoperation matrix

$$D = \{D_{ij}\}, \quad D_{ij} = \begin{cases} d_{ij} & i,j \notin \rho \\ \delta & j \in \rho, i = 1,\dots,m \\ d_{1j} & i \in \rho, j \notin \rho \end{cases} \tag{5}$$

For manually operated switches, the travelling time d_{ij} is clearly related to the topographic path covered by the crew in the route between switches i and j. We define $R_{ij} = (Y, \Delta)$ as a tuple, where $Y = \{i,\dots,y,\dots,j\}$ is the set of switches covered by the operation crew in the route between switches i and j, and $\Delta = \{0,\dots,d_{iy},\dots,d_{ij}\}$ is the set of the corresponding travelling times.

E. Asymptotic reliability of power delivery

The unavailability of the elements follows from the definitions above

$$U = \lambda \cdot l + (\lambda r) \cdot K \tag{6}$$

where $\cdot$ denotes a vector or matrix multiplication and other multiplications are element by element. The down times including no or unstable power supply become

$$\tau = \frac{U}{\lambda \cdot 1_m} \tag{7}$$

where 1_m is a vector with m ones. If we regard an element as available also when it is working but unstable we get

$$U^* = \lambda \cdot L^* + (\lambda r) \cdot K \tag{8}$$

and correspondingly the element down times

$$\tau^* = \frac{U^*}{\lambda \cdot 1_m} \tag{9}$$

This is the accepted version of an article published at 2021 5th International Conference on System Reliability and Safety (ICSRS)
http://dx.doi.org/10.1109/ICSRS53853.2021.9660625

From equations (6) and (8) it can be observed that, if $r = 0$, location time, outage time and their respective unavailabilities present a linear relationship. For this reason, fault location and outage time reduction and unavailability reduction are used interchangeably in the paper.

IV. Entropy based fault localization and isolation

The basic idea is to establish a plan for localization of the failed network element as fast as possible and therefore to reduce the power unavailability associated with a network failure. This is done by maximizing the information about where the failure is located by each switch operation. This plan is represented by a binary tree B. The details on building the tree are presented in Subsection IV-A. Based on the tree, measures of the times without power delivery under the localization procedure may be obtained. This is presented in Subsection IV-B.

A. Building the decision tree

Let $k = \{k_i\}$ be a vector that identifies the potentially faulty elements, where $k_i = 0$ indicates that element i is known to be fault free and $k_i = 1$ indicates that it may be faulty. At the initial stage, immediately after a fault is detected and the breaker opens, $k = \{1, 1, \ldots, 1\}$; the repairing crew is considered located alongside the breaker ($i_{\text{prev}} = 1$), and the binary decision tree is an empty graph $B = \emptyset$. The vector k is stored in the list X, which represents the list of subnets to be inspected for further expansion of the tree. Given k, by exploiting the principles on entropy presented in Section II, the switch i_{open} that minimizes the expected entropy $J_i(k)$ is identified through (10):

$$i_{\text{open}} = \text{argmin}_i J_i(k) \tag{10}$$

where, using (1) and the properties of logarithms:

$$\begin{aligned} J_i(k) &= \frac{(\lambda K_i)\cdot k}{\lambda \cdot k}\mathscr{E}\left(\frac{\lambda K_i k}{(\lambda K_i)\cdot k}\right) + \frac{(\lambda \overline{K}_i)\cdot k}{\lambda \cdot k}\mathscr{E}\left(\frac{\lambda \overline{K}_i k}{(\lambda \overline{K}_i)\cdot k}\right) \\ &= \mathscr{E}\left(\frac{\lambda k}{\lambda \cdot k}\right) - \mathscr{E}\left(\frac{(\{K_i, \overline{K}_i\}\lambda)\cdot k}{\lambda \cdot k}\right) \end{aligned} \tag{11}$$

The first term of (11) is constant under the argmin operation and may be neglected.

The overall procedure is summarized through pseudo-code in Algorithm 1, where the above mentioned initial conditions are formalized in Line 1.2. Due to the assumptions highlighted in Subsection III-D, the remotely controlled switches are prioritized to manual switches operation and are always inspected first (Lines 1.3-1.7). Remotely controlled switches represent therefore the immediate options in the decision tree building process, whereas the rest of the tree is formed by the best sequences of manual switches operation (Lines 1.8-1.14).

For each iteration, first the equation (10) is calculated (Lines 1.4 and 1.9), which provides the candidate switch to be opened with the maximum entropy decrease. For the manually operated switches, since the on-route switches between i_{prev} and i^*_{open} may provide further knowledge to the fault location with no additional traveling time, the closest switch on the route is operated first (Line 1.10). Moreover, after each computation over the manually operated switches, the repairing crew moves from i_{prev} to i_{open} (Line 1.12).

After the inspection, the decision tree is updated (Lines 1.5 and 1.11).

The decision tree updating function is detailed in Algorithm 2. First, two edges are built, $k \mapsto kK_{i_{\text{open}}}$ and $k \mapsto k\overline{K}_{i_{\text{open}}}$, where $kK_{i_{\text{open}}}$ and $k\overline{K}_{i_{\text{open}}}$ represent respectively the downstream and not-downstream subnet of the operated switch i_{open}. The property $(i_{\text{open}}, D_{i_{\text{prev}} i_{\text{open}}})$ is stored alongside the edges, where $D_{i_{\text{prev}} i_{\text{open}}}$ represents the switch operation time of i_{open} from i_{prev} (Line 2.2; see subsection III-D for reference). These edges are then attached to the decision tree B in Line 2.3.

In Line 2.4 the vector of branches to be further inspected are updated. The current branch k is removed, and the branches representing the downstream ($kK_{i_{\text{open}}}$) and not-downstream ($k\overline{K}_{i_{\text{open}}}$) subnets of the operated switch i_{open} are added, unless they represent a single element ($k \cdot K_{i_{\text{open}}} = 1$). This overall process is run iteratively in Algorithm 1 over the list of subnets stored in the vector X (Lines 1.6 and 1.13). A new subnet k is popped out from the vector X and analysed until X is empty (Line 1.8), i.e. the whole network is investigated and all the possible fault locations are analysed.

Algorithm 1 Entropy Based Function - EBF

1.1: **function** EBF(K, ρ)
1.2: **set** $i_{\text{prev}} = 1, k = 1_m, B = \emptyset, X = \{[k]\}$
1.3: **while** $\rho \cdot k > 1$ **do**
1.4: $i_{\text{open}} = \text{argmin}_{i \in \rho k}(J_i(k))$
1.5: $X, B = DTUF(K, k, i_{open}, i_{prev}, D, B, X)$ ▷ Alg. 2
1.6: $k = \textbf{pop}(X \wedge (\rho \cdot x > 1))$
1.7: **end while**
1.8: **while** $X \neq \emptyset$ **do**
1.9: $i^*_{\text{open}} = \text{argmin}_i(J_i(k))$
1.10: $i_{\text{open}} = y \mid (d_{i_{\text{prev}} y} = \min_{y \neq i_{\text{prev}}}(\Delta), \Delta \in R_{i_{\text{prev}} i_{\text{open}^*}})$
1.11: $X, B = DTUF(K, k, i_{open}, i_{prev}, D, B, X)$ ▷ Alg. 2
1.12: **set** $i_{\text{prev}} = i_{\text{open}}$
1.13: $k = \textbf{pop}(X)$
1.14: **end while**
1.15: **return** B
1.16: **end function**

Algorithm 2 Decision Tree Updating Function - DTUF

2.1: **function** DTUF($K, k, i_{\text{open}}, i_{\text{prev}}, D, B, X$)
2.2: $(k \mapsto kK_{i_{\text{open}}}), (k \mapsto k\overline{K}_{i_{\text{open}}}) := (i_{\text{open}}, D_{i_{\text{prev}} i_{\text{open}}})$
2.3: $B := B \cup (k \mapsto kK_{i_{\text{open}}}) \cup (k \mapsto k\overline{K}_{i_{\text{open}}})$
2.4: $X := X \cup (\textbf{If } k \cdot K_{i_{\text{open}}} > 1 \textbf{ then } kK_{i_{\text{open}}} \textbf{ else } \emptyset) \cup (\textbf{If } k \cdot \overline{K}_{i_{\text{open}}} > 1 \textbf{ then } k\overline{K}_{i_{\text{open}}} \textbf{ else } \emptyset) \setminus k$
2.5: **return** X, B
2.6: **end function**

This is the accepted version of an article published at 2021 5th International Conference on System Reliability and Safety (ICSRS)
http://dx.doi.org/10.1109/ICSRS53853.2021.9660625

B. Fault localization and power recovery times

The tree B may be used to obtain the fault localization times. It is seen that

$$l = \{\mathscr{G}_{\text{dist}}(B; 1_m, k^{(i)})\}_{i=1,\ldots,m} \tag{12}$$

where $\mathscr{G}_{\text{dist}}(B;x,y)$ is the distance (sum of the edge weights D_{ij}) from vertex x to y in B.

To find the time from element i fails and until element j may either be put into unstable operation, l^*_{ij}, a two step procedure is applied. First, the time, $\tilde{l}_{ij}$ from the search procedure starts until it is concluded that element j is in another branch of the tree than the failed element i. Second, element j cannot be powered before all upstream elements of j, i.e. $x \in K^u_j$ where $\{K^u_1, \ldots, K^u_m\}^T = K - I_m$, are also in other branches than the failed i. Hence,

$$l^*_{ij} = \max_{\forall x \in K^u_j} (\tilde{l}_{ij}, \tilde{l}_{ix}) \tag{13}$$

To obtain the time $\tilde{l}_{ij}$, the common path in the decision graph B is used. However, we must include the first time after the branches split, in order to include the time it takes to operate the switch. Hence, the length of the joint path plus one is first obtained.

$$\ell_{ij} = |\, \mathscr{G}_{\text{path}}(B; 1_m, k^{(i)}) \cap \mathscr{G}_{\text{path}}(B; 1_m, k^{(j)}) \,| + \mathbb{1}(i \neq j) \tag{14}$$

When the element i is faulty, element j is recognized as fault free when node ℓ_{ij} along the search path $\mathscr{G}_{\text{path}}(B; 1_m, k^{(i)})$ is reached and we get

$$\tilde{l}_{ij} = \mathscr{G}_{\text{dist}}(B; 1_m, \mathscr{G}_{\text{path}}(B; 1_m, k^{(i)})_{\ell_{ij}}) \tag{15}$$

where $\mathscr{G}_{\text{path}}(B; 1_m, k^{(i)})_{\ell_{ij}}$ is the ℓ_{ij}th element of the path. Comparing the results obtained from (12) and (13), it is seen that $l = L^* \cdot I_n$ and that $l^*_{ij} \leq l_i$ as pointed out in Subsection III-C.

V. Introducing fault indicators

A. Model of fault indicators

To speed up the fault localization process, fault indicators may be introduced. The fault indication is represented with a vector $a = \{a_1, \ldots, a_m\}$, where $a_i = 1$ indicates that a fault is detected in the downstream power flow of component i, $a_i = 0$ indicates that *no* fault is detected and $a_i = \phi$ that no indicator is present at element i.

Fault indicators can fail themselves. Only passive failures are considered, i.e. false negative $a_i = 0$ when there is a fault. The reason for this is that active failures, i.e. false positives $a_i = 1$ when there is no fault, are identifiable and rectifiable during normal operation. It is assumed that indicator failures occur independently with probabilities α_i. Since the breaker is always reacting on a power system fault, the associated fault indicator is always working, i.e., $\alpha_1 = 0$. The fault indicators' failure probabilities are represented by the vector $\alpha = \{\alpha_1, \ldots, \alpha_m\}$.

In the calculations in Subsections V-B and V-C we need the probability of a series of consecutively failing fault indicators. To simplify, we establish a vector $\alpha^c = \{\alpha^c_1, \ldots, \alpha^c_m\}$ where each element is the probability that the indicator has failed, as well as all indicators between the root (breaker) and the indicator, i.e.

$$\alpha^c_i = \prod_{\forall j: K^T_{ij}=1} (K \cdot \alpha)^T_{ij} \tag{16}$$

B. Dominant sets of fault indicator vectors

For each element fault, the number of feasible fault indicator vectors grows exponentially with the number of indicators between the breaker and the the fault. Fortunately, it is not necessary to deal with the individual fault indicator vectors. Since there will always be a downstream power fault of element i when $a_i = 1$, it is the last indicator with positive indication that is relevant for the location. All fault indicator vectors having this property are said to belong to the same dominant set $\mathscr{A}_j$. Formally:

$$\mathscr{A}_j = a \mid (a \cdot K_j)_i = \begin{cases} 1 & i = j \\ 0 \wedge \phi & \text{Otherwise} \end{cases} \tag{17}$$

It is seen that the number of dominant sets are the same as the number of fault indicators in the system, $m - |a : a_i = \phi|$ and, as will be shown below, it is only necessary to investigate the system for these. Dominant sets defined by fault indicators assigned to leaf nodes of the graph G associated with the network represent completely identified faults.

The dominant set $\mathscr{A}_j$ contains all feasible combinations of fault indicators between j and the root. Hence, the probability of the set conditioned by the fault being in element i is given by the fault indicator j working and the following up to and including i failed. Using (16), it is obtained

$$P(\mathscr{A}_j \mid i) = \begin{cases} (1-\alpha_j)\frac{\alpha^c_i}{\alpha^c_j} & K_{ji} = 1 \\ 0 & \text{Otherwise} \end{cases} \tag{18}$$

From which it follows that

$$P(\mathscr{A}_j) = \sum_{i=1}^{m} P(\mathscr{A}_j \mid i)\, \frac{\lambda_i}{\lambda \cdot 1_m} \tag{19}$$

C. Fault intensity for a given dominant set

When a fault occurs and we get a fault indicator vector $a \in \mathscr{A}_j$ we know that the fault is in the subtree below element j. To build a search tree for this subtree along the procedure of Section IV, the prior fault intensities λ should be modified taking into account the fault indicator failure probabilities α. The fault intensity of element j will not be affected. The fault intensity of the next element, say x, will be reduced by α_x, the following one, say y, by $\alpha_x\alpha_y$ and so on, to account for the fraction of faults not detected. In general:

$$\lambda^{(\mathscr{A}_j)} = K_j(1-\alpha_j)\frac{\alpha^c}{\alpha^c_j}\lambda \tag{20}$$

The posterior failure probabilities of the vectors a become $P(i_{\text{failed}} \mid \mathscr{A}_j) = \lambda_i^{(\mathscr{A}_j)} / (\lambda^{(\mathscr{A}_j)} \cdot 1_m)$. Hence, by using $\lambda^{(\mathscr{A}_j)}$ instead of λ in the search procedure in Section IV, we may obtain the binary tree decision tree $B^{(\mathscr{A}_j)}$ that includes the information from the indicators.

This is the accepted version of an article published at 2021 5th International Conference on System Reliability and Safety (ICSRS)
http://dx.doi.org/10.1109/ICSRS53853.2021.9660625

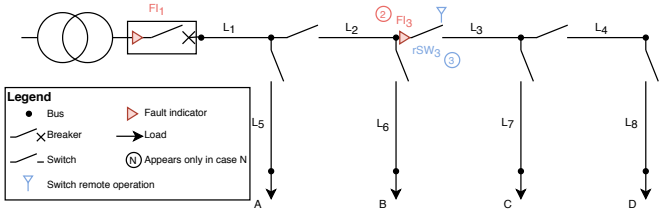

Fig. 2. 8-bus radial distribution network.

D. Asymptotic reliability of power delivery with fault indicators

The results obtained in Section III-E may be extended to a system with fault indicators. Since only one dominant set will occur at a time, the system unavailability will be the sum of the contributions from each of these. The fault localization and power recovery times in Subsection IV-B may be obtained for each set $\mathscr{A}_j$ by using $B^{(\mathscr{A}_j)}$ instead of B in (12), (14) and (15), yielding $l^{(\mathscr{A}_j)}$ and $L^{(\mathscr{A}_j)*}$. The fault intensities are given in (20). Substituting the altered fault location times due to the fault indicators into (6) to (9) we obtain

$$\begin{aligned} U &= \sum_{\forall j} \lambda^{(\mathscr{A}_j)} l^{(\mathscr{A}_j)} + (\lambda r)\cdot K, \qquad \tau = \frac{U}{\lambda \cdot 1_m} \\ U^* &= \sum_{\forall j} \lambda^{(\mathscr{A}_j)} \cdot L^{(\mathscr{A}_j)*} + (\lambda r)\cdot K, \qquad \tau^* = \frac{U^*}{\lambda \cdot 1_m} \end{aligned} \tag{21}$$

VI. Examples

The method is illustrated through two main examples. In subsection VI-A, an 8-branches distribution network is analysed with three main configurations: without automation devices, with one fault indicator, and with one remotely controlled switch. The network unavailability is analysed in terms of yearly fault location time and outage time by considering the fault intensities on the 8 network branches. In the second example a specific fault location is analyses, by considering the case of correct fault detection from the fault indicator, and the case when the fault indicator provides a wrong information to the DSO.

A. Example 1

The network analysed is represented in Fig. 2. Each branch may be disconnected by a switch. By default, it is assumed that the breaker at bus 1 is integrated with a fault indicator (FI_1). The sectioning time is given either by $\delta = 1s$ in case of remotely controlled switches, or the time required by the crew to reach the substation in case of manually operated switches. This latter time is proportional to the distance covered by the crew (a crew motion speed of 30 km/h is considered, which travels alongside the feeder). The intrinsic time to manoeuvre the switches is assumed to be zero for simplicity. The line segments lengths are chosen with a probability distribution that describes a typical urban scenario [11]. The failure rates of the network branches are drawn from an uniform distribution between 0.01 and 0.03 failures per km a year. For simplicity,

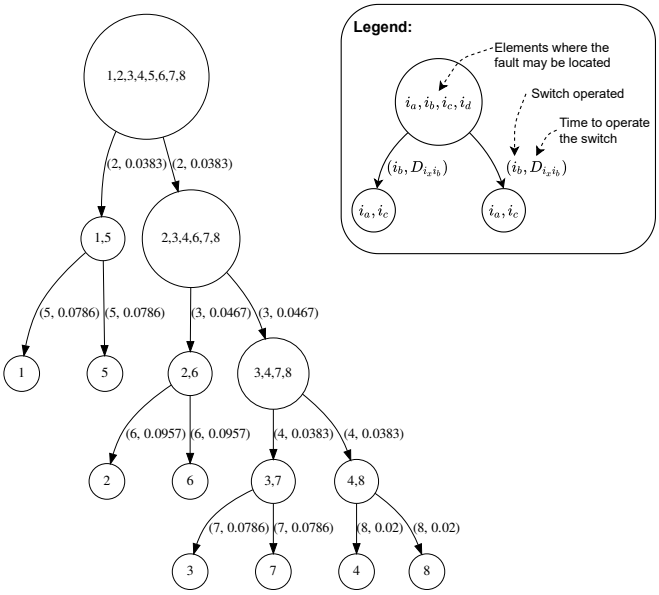

Fig. 3. Binary tree - Example 1, Case 1 - Manual switches, no failure detectors except at the breaker

only the faults occurring on the lines are considered, and the loads reliability is not included in the analysis. Three cases will be analysed:

1) Default network configuration: all branches may be disconnected by manual switches, and no fault indicators are available except from the ideal one at the HV/MV substation (FI_1);
2) Fault indicator at line L3 (FI_3): the line L3 departs from a switch equipped with a fault indicator, that detects fault currents downstream of SW3;
3) Remotely controlled switch at line L3 (rSW_3): the line L3 departs from a switch that is remotely controlled by the operators (rSW_3).

All the fault indicators are characterized by an intrinsic failure rate $\alpha = 0.01$. An exception is represented by the Fault Indicator FI_1, that is assumed to be perfect ($\alpha_1 = 0$).

a) Case 1: Without fault indicators, only one binary tree is generated, see Fig. 3, which returns the quickest localization of the fault given both the failure rates and the sectioning time due to the travel distances between the switches.

b) Case 2: As explained in Subsection V-C, two binary decision trees are obtained, corresponding to the two dominant sets, see Fig. 4. Fig. 4a covers the cases when the output of FI_3 is equal to 0: the fault is either not downstream of FI_3, or the fault is downstream of FI_3, but the fault indicator is failed. Fig. 4b covers the cases when output of FI_3 is equal to 1. It can be observed the different sequence of switching in Fig. 4a compared with Case 1 (Fig. 3), which is due to the low probability ($\alpha_3 = 0.01$) of failure downstream of FI_3.

c) Case 3: The tree in Fig. 5 shows that the remote operation of the switch at the head of line L3 takes place first (cf. Algorithm 1) and the manual search takes place in the part of the network where the fault is located by this operation.

This is the accepted version of an article published at 2021 5th International Conference on System Reliability and Safety (ICSRS)
http://dx.doi.org/10.1109/ICSRS53853.2021.9660625

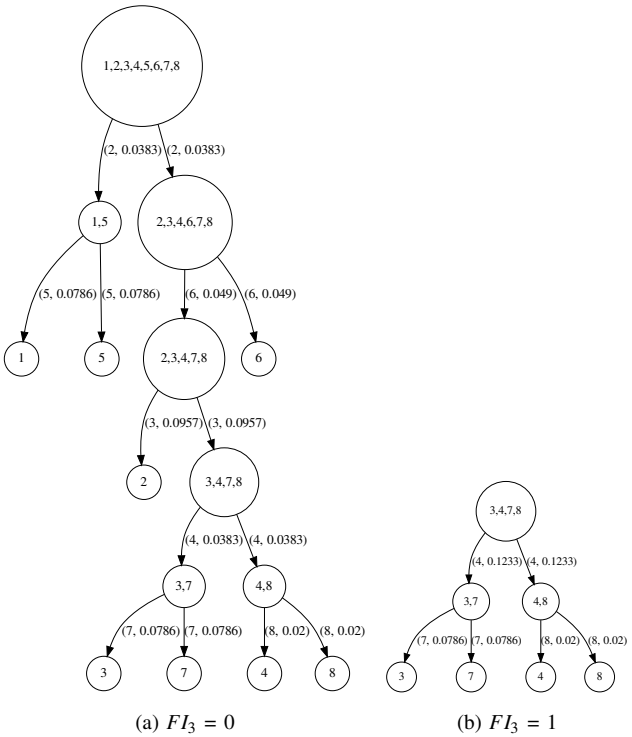

(a) $FI_3 = 0$ (b) $FI_3 = 1$

Fig. 4. Binary tree - Example 1, Case 2 - Imperfect fault indicator that monitors line L3

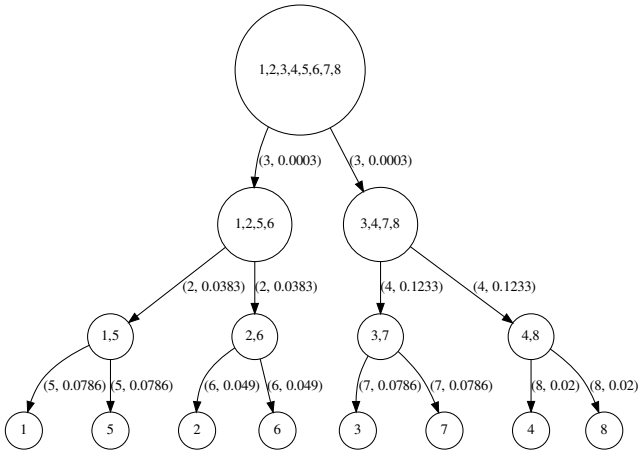

Fig. 5. Binary tree - Example 1, Case 3 - Remotely operated switch at the head of line L3

TABLE I
UNAVAILABILITY IN TERMS OF YEARLY AVERAGE FAULT LOCALIZATION TIME AND OUTAGE TIME [H] OF THE 8-BUS DISTRIBUTION NETWORK

	Case 1	Case 2	Case 3
Fault localization time [h], τ	9.317	8.842	8.446
Outage time [h], τ^*	7.119	5.751	5.448

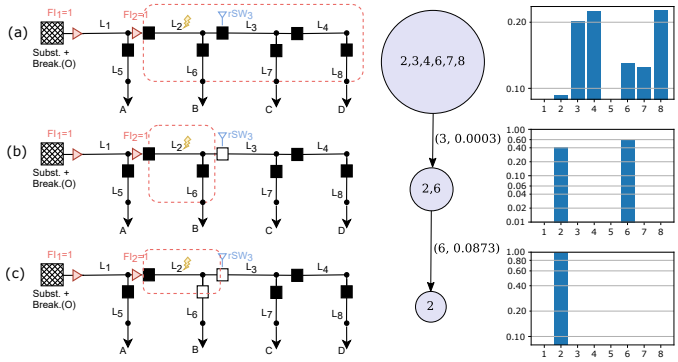

Fig. 6. Example 2, Case 1 - Sequence of switches operation and distribution of fault location probabilities when $FI_2 = 1$

In Table I the unavailability due to fault location and isolation – i.e., repair time $r = 0$ in (6), (8) and (21) – of the three cases are reported. They are presented in terms of yearly average fault localization time τ (only stable operation) and outage time τ^* (unstable operation accepted). The installation of automation devices results in a significant improvement. A slight gain can be observed when installing the remotely controlled switch (Case 3), compared with the case where the fault indicator is in place (Case 2). It is caused by the remotely controlled switch behaving equivalently to a perfect fault indicator. The similarity is due to no travel time being saved by remote operation with the faults downstream of the failure indicator in the given topology, and the low failure probability (0.01) of the failure indicator.

B. Example 2

The three cases described in the previous subsection have shown how, known the failure intensities, the network topology, the placement of the automation devices and the uncertainty of the information, with the entropy method it is possible to build a strategy for reducing the unavailability associated with a fault inspection.

In this subsection a specific fault condition will be analysed. The network is the 8-branches distribution network already analysed in the previous example. In this specific case, the fault indicator is placed on line L2 (FI_2), whereas the remotely controlled switch is placed on line L3 (rSW_3). The fault is considered occurring on line L2.

Two cases will be analysed:

- the fault indicator FI_2 correctly detects the fault occurring downstream;
- the fault indicator FI_2 does not detect the fault.

a) Case 1: The sequence of switches operation for locating the fault is shown in Fig. 6. For graphical representation simplicity, all the binary tree nodes not interesting for this specific fault location are not shown in the figure. It can be observed the distribution of probabilities of fault location, due to the different failure intensities across the different branches and the information obtained by FI_2, which returns a probability of fault location on lines L1 and L5 equal to

This is the accepted version of an article published at 2021 5th International Conference on System Reliability and Safety (ICSRS)
http://dx.doi.org/10.1109/ICSRS53853.2021.9660625

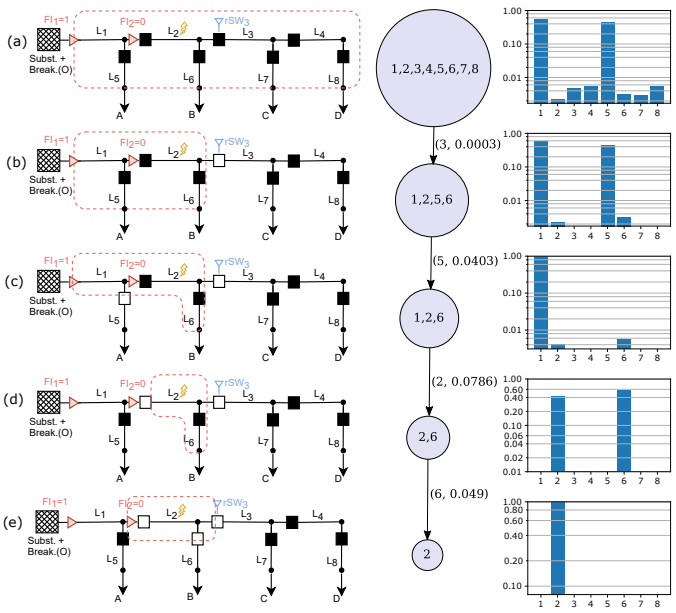

Fig. 7. Example 2, Case 2 - Sequence of switches operation and distribution of fault location probabilities when $FI_2 = 0$

0 (Fig. 6a). According to the assumptions of Section III-D, the remotely controlled switch rSW_3 is prioritized in the operation. After operating the switch, the fault is immediately identified being upstream of rSW_3, therefore the investigation is restricted to the subnet {L2, L6} (Fig. 6b). The fault is finally located by operating the switch on line L6 (Fig. 6c).

b) Case 2: In Fig. 7 it is represented the sequence of switches operation that result from an incorrect information from the fault indicator FI_2. After the breaker opening, since $FI_2 = 0$, all the network lines are candidate for being affected by the fault (Fig. 7a). Being $FI_2 = 0$, the probability distribution returns a high probability of the faults being on lines L1 and L5, i.e. upstream of FI_2(Fig. 7b), meanwhile the probabilities of the failure being downstream of FI_2 are negligible. Therefore, after the prioritized operation of rSW_5, the inspection continues with the operation on switch on line L5 (Fig. 7c), the operation on switch on line L2 (Fig. 7d) identifies the fault being downstream of FI_2. The operation over the switch on line L6 uniquely identifies the fault on line L2.

VII. Case Studies

The method has been applied for analysing the impact of an increasing number of automation devices on three standard radial distribution networks. For data and topology of the chosen networks, cf. [12]–[14]. For each of these, 16 automation modes are investigated, i.e. all combinations of the number of fault indicators and remotely controlled switches densities of Table II.

The automation devices placement is carried out prioritizing the buses that present the highest outer-degree, i.e. the buses that feed the largest number of lines are those primarily

TABLE II
Radial network configurations studied

Parameters	Values (x)
Networks [12]–[14]	69, 85, 141 $[N_{\text{buses}}]$
Remotely controlled switches	$[0, 1/10, 1/6, 1/3] \times N_{\text{lines}}$
Fault indicators	$[0, 1/10, 1/6, 1/3] \times N_{\text{lines}}$

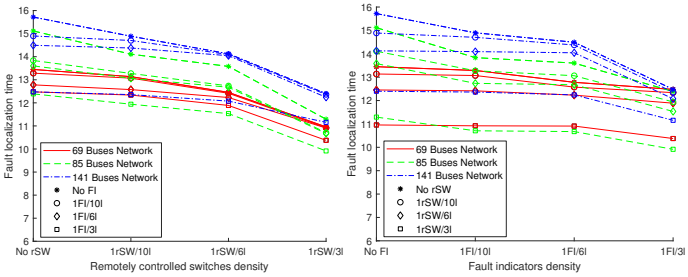

(a) Remotely controlled switches (b) Fault indicators

Fig. 8. Unavailability (U) in terms of average fault location time per year

provided with automation devices in an decreasing order. When the number of buses of the selected degree is bigger than the number of devices, the devices are randomly placed over these buses. The lines not equipped with remotely controlled switches are sectionable with manually operated switches. The same assumptions taken in Section VI regarding operation time for manually and remotely operated switches, as well as lines failure rates, are also adopted in the present case studies.

The calculations analyze how the unavailability (in terms of average fault location time and fault outage time) vary when increasing the number of automation devices. The results are reported in Fig. 8, which shows the variation in terms of fault location time, and Fig. 9, which shows the variation in terms of fault outage time. What can be observed from these figures is that the highest reduction in the fault location and fault outage time are obtained by increasing the remotely controlled switches. For instance, it is seen in Fig. 9 that in the case of the 85 buses network, the placement of 1 remotely controlled switches every 10 lines gives a reduction in terms of average outage time significantly lower than the case where 1 fault indicator every 10 lines is introduced.

The results shown in Fig. 8 and Fig. 9 stem from a single

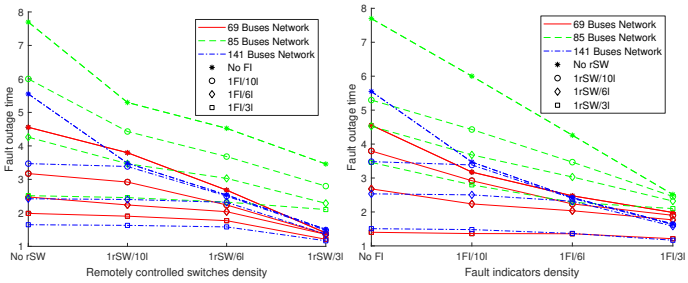

(a) Remotely controlled switches (b) Fault indicators

Fig. 9. Unavailability of power (U^*) in terms of average outage time per year

This is the accepted version of an article published at 2021 5th International Conference on System Reliability and Safety (ICSRS)
http://dx.doi.org/10.1109/ICSRS53853.2021.9660625

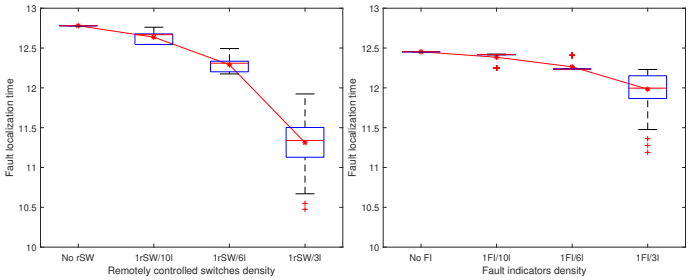

(a) Fixed 1/6 fault indicators; random remote switches

(b) Random fault indicators; Fixed 1/6 remote switches

Fig. 10. Sensitivity analysis of unavailability (U) in terms of average fault location time per year

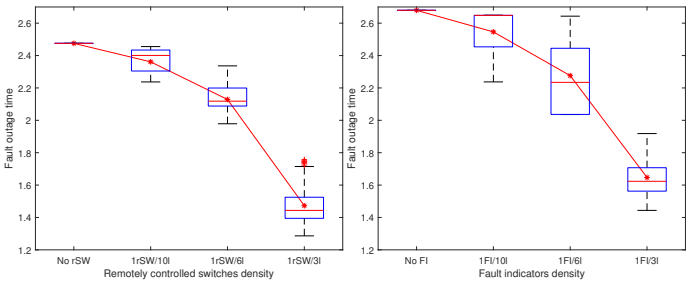

(a) Fixed 1/6 fault indicators; random remote switches

(b) Random fault indicators; fixed 1/6 remote switches

Fig. 11. Sensitivity analysis of unavailability of power (U^*) in terms of average outage time per year

random placement of devices. To generalize the results, a sensitivity analysis has been carried out for the 69 buses network, where each random placement has been repeated 100 times. An analysis has been performed with keeping a constant placement of 1 fault indicator every 6 lines, and by randomly varying the placement of remotely controlled switches. The results are shown in Fig.s 10a and 11a for the fault outage time. In Fig. 10b and Fig. 11b the results of the analogous analysis when varying the placement of fault indicators with a constant placement of 1 remotely controlled switch every 6 lines are shown. Fig. 10 confirms that the largest decrease in location time is obtained by increasing the number of remote switches. Increasing the number of fault indicators yield a marginal effect. The sensitivity to device placement as indicated by the box-plots yield some interesting observations:

- The sensitivity to the placement of devices is larger for outage time (U^*) than the location time (U).
- With a careful (optimal) placement of a high density of devices, a considerable reduction in unavailability may be achieved, cf. the low outliers for 1rSW/3l and 1FI/3l in Fig.s 10a and 10b respectively. The corresponding lower bar of Fig. 11 indicates the same.
- For the middle range of devices, i.e. one per six and one per ten, the random placement shows a overlap, and the saving coming from a good planning can be significant, especially with respect to outage time (U^*).

TABLE III
COMPUTATION DURATION (MEAN ± STD. DEV) FOR DIFFERENT DISTRIBUTION NETWORKS AND FAULT INDICATOR DENSITIES

	69 buses [12]	85 buses [13]	141 buses [14]
No FI	46.2 ± 2.46ms	70.1 ± 2.54ms	229 ± 3.53ms
1FI/3l	209 ± 5.4ms	267 ± 2.69ms	1090 ± 5.63ms

Table III shows the computation times for the three networks with no fault indicators and networks with 1 fault indicator every three lines. The algorithm is coded in Python (v.3.6.8), and runs on an Windows 10 on a DELL OptiPlex 7050 machine with Intel i7-7700 quadcore CPU and 32GB of RAM. Numbers are based on 700 replications. It can be observed a general increase in terms of computation duration when both fault indicator density and network size increase. With networks with comparable size (like 69 and 85 buses network), comparing the cases with no automation and with fault indicators the increase shows a not proportional behaviour. It is explained by additional factors that contribute to the complexity of the problem, such as the topology of the network. The algorithm provides results in about 1 second even for the most complex network and automation setup analyzed. Hence, it is sufficiently fast to allow interactive planning of large networks as well as optimization based on iterative heuristics.

VIII. CONCLUSION

In this paper a novel method for fault location and isolation has been presented. The algorithm consists of building a binary decision tree based on the principle of entropy minimization, which returns the switching sequence that optimizes the average number of inspections in fault location.

The application of the method to different network topologies with different levels of automation (in terms of fault indicators and remotely controlled switches placement) shows the capability to support operators in optimal strategies for fault location and isolation, and to conduct analysis over the impact of an increasing automation towards the availability of the power system. Finally, the computational efficiency of the algorithm was presented, which validates the potential of the method for being used within planning optimization methods.

REFERENCES

[1] A. Bahmanyar, S. Jamali, A. Estebsari, and E. Bompard, "A comparison framework for distribution system outage and fault location methods," *Electric Power Systems Research*, vol. 145, pp. 19–34, Apr. 2017.

[2] M. Shafiullah and M. A. Abido, "A Review on Distribution Grid Fault Location Techniques," *Electric Power Components and Systems*, vol. 45, no. 8, pp. 807–824, May 2017.

[3] S. S. Gururajapathy, H. Mokhlis, and H. A. Illias, "Fault location and detection techniques in power distribution systems with distributed generation: A review," *Renewable and Sustainable Energy Reviews*, vol. 74, pp. 949–958, Jul. 2017.

[4] T. S. Hermansen, H. Vefsnmo, K. A. Tutvedt, H. Nett, S. Simonsen, and G. Kjølle, "Reliability analysis methodology for smart fault handling in mv distribution grids," in *CIRED 2019*, Madrid, Spain, Jun. 2019, p. 5.

[5] A. Janjic and L. Velimirovic, "Integrated fault location and isolation strategy in distribution networks using Markov decision process," *Electric Power Systems Research*, vol. 180, p. 106172, Mar. 2020.

This is the accepted version of an article published at 2021 5th International Conference on System Reliability and Safety (ICSRS)
http://dx.doi.org/10.1109/ICSRS53853.2021.9660625

[6] J. N. Kapur and H. K. Kesavan, "Entropy optimization principles and their applications," in *Entropy and energy dissipation in water resources*. Springer, 1992, pp. 3–20.

[7] A. Leon-Garcia and A. Leon-Garcia, *Probability, statistics, and random processes for electrical engineering*, 3rd ed. Upper Saddle River, NJ: Pearson/Prentice Hall, 2008, oCLC: ocn181079252.

[8] T. M. Cover and J. A. Thomas, *Elements of information theory*, 2nd ed. Hoboken, N.J: Wiley-Interscience, 2006, oCLC: ocm59879802.

[9] J. R. Quinlan, "Induction of decision trees," *Mach Learn*, vol. 1, no. 1, pp. 81–106, Mar. 1986.

[10] A. Brutzkus, A. Daniely, and E. Malach, "On the Optimality of Trees Generated by ID3," *arXiv:1907.05444 [cs, stat]*, Jul. 2019, arXiv: 1907.05444.

[11] S. Abeysinghe, J. Wu, M. Sooriyabandara, M. Abeysekera, T. Xu, and C. Wang, "Topological properties of medium voltage electricity distribution networks," *Applied Energy*, vol. 210, pp. 1101–1112, Jan. 2018.

[12] D. Das, "Optimal placement of capacitors in radial distribution system using a Fuzzy-GA method," *International Journal of Electrical Power & Energy Systems*, vol. 30, no. 6, pp. 361–367, Jul. 2008.

[13] D. Das, D. P. Kothari, and A. Kalam, "Simple and efficient method for load flow solution of radial distribution networks," *International Journal of Electrical Power & Energy Systems*, vol. 17, no. 5, pp. 335–346, Oct. 1995.

[14] H. M. Khodr, F. G. Olsina, P. M. D. O.-D. Jesus, and J. M. Yusta, "Maximum savings approach for location and sizing of capacitors in distribution systems," *Electric Power Systems Research*, vol. 78, no. 7, pp. 1192–1203, Jul. 2008.

This is the accepted version of an article published at 2021 5th International Conference on System Reliability and Safety (ICSRS)
http://dx.doi.org/10.1109/ICSRS53853.2021.9660625